Front. Mech. Eng. 2012, 7(2): 219–230
DOI 10.1007/s11465-012-0320-9

RESEARCH ARTICLE

Kejia LI, Xilun DING, Marco CECCARELL

A total torque index for dynamic performance evaluation of a radial symmetric six-legged robot

Abstract This article focuses on the dynamic index and performance of a radial symmetric six-legged robot. At first the structure of the robot is described in brief and its inverse kinematics is presented. Then the dynamic model is formulated as based on the Lagrange equations. A novel index of total torque is proposed by considering the posture of the supporting legs. The new index can be used to optimize the leg's structure and operation for consuming minimum power and avoiding unstable postures of the robot. A characterization of the proposed six-legged robot is obtained by a parametric analysis of robot performance through simulation using the presented dynamic model. Main influences are outlined as well as the usefulness of the proposed performance index.

Keywords six-legged robots, dynamic modeling, performance index

1 Introduction

One of the most significant advantages of six-legged robot refers to its high locomotion ability. Legged robots can walk through rough terrain, especially in the outdoor environments, rather than other types of mobile robots. In order to improve the performance of six-legged robots, dynamic analysis becomes a key research issue, and it is very important for mechanical optimization design and leg operation of six-legged robot.

To analyze the dynamic performance of six-legged robots, a dynamic model is necessary. Contributions have been made by several authors in the area of dynamic modeling and performance analysis of the multi-legged robot. Chen et al. established the dynamic equations of multi-legged robot in a modular method [1]. Barreto et al. used the free body diagram method to obtain the dynamic model of a six-legged robot [2]. Yiu et al. studied the dynamics of parallel manipulators in Ref. [3]. Ding et al. analyzed the dynamics of hexapod robot with elastic joints using screw theory [4]. For the dynamic performance of the multi-legged robot, Silva et al. proposed four dynamic indices in the aspect of energy and power [5]. Bowling had analyzed the performance of legged robots by examining the kinematic constraints associated with ground contact in Refs. [6,7]. Erden handled with the distribution of required forces and moments to the supporting legs by the method of torque-distribution [8]. Low and Bai introduced an index named terrain complexity based on the terrain evaluation [9,10]. However, the existing indices of robot's dynamic performance which minimize the power consumed have no consideration on stability reduction effect.

In this paper, an index T_{tot} of total torque is proposed by considering the posture of supporting legs. The new index T_{tot} can be used to optimize the leg's structure and operation for consuming the minimum power and avoiding the unexpected postures that the supporting legs can reduce the stability excessively. The effects of four parameters (length of leg, mass distribution of leg, step length and joint angles of supporting legs in standing state) on the dynamic performance are analyzed quantitatively as based on dynamic equations. The analyses of leg operation in two cases are presented as based on the index T_{tot}.

The rest part of this paper is organized as follows. In Sect. 2, radial symmetric six-legged robot and its inverse kinematics are described. In Sect. 3 the dynamic modeling of this robot is presented. An index of total torque considering the posture of supporting legs is proposed in Sect. 4. The robot's dynamic performance is analyzed by simulation experiments in Sect. 5. Finally, a conclusion is summarized in Sect. 6.

Received January 6, 2012; accepted March 10, 2012

Kejia LI (✉), Xilun DING
Robotics Institute, School of Mechanical Engineering and Automation, Beijing University of Aeronautics and Astronautics, Beijing 100191, China
E-mail: likejia5@gmail.com

Marco CECCARELL
Laboratory of Robotics and Mechatronics, University of Cassino, 03043 Cassino, Italy

2 Structure and inverse kinematics of the six-legged robot

2.1 Structure of the robot

Different with the hexapod robots in Refs. [11–14], the six-legged robot we proposed is radial symmetric. The mechanical structure is composed of six leg subsystems and the body with hemispheric shell as shown in Fig. 1. The radius of body is 300 mm, and the length of leg is 600 mm. Each leg is composed of hip, thigh and calf. The mass of robot is evenly distributed, and the mass center of each part is located at its geometric center.

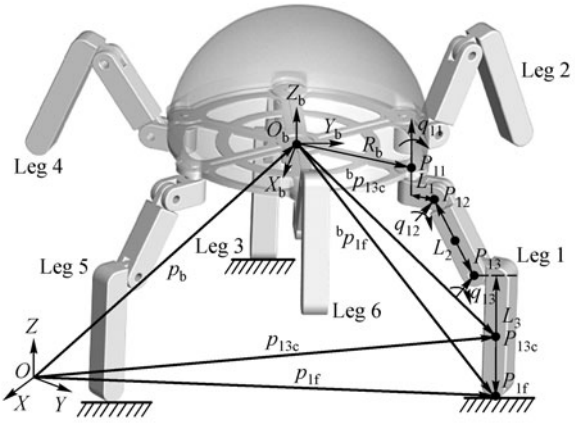

Fig. 1 The radial symmetric six-legged robot

Since the legs are located symmetrically, the angle between adjacent legs is 60°. There are three joints in each leg, namely hip yawing joint, hip pitching joint and knee joint. All of the joints are driven by DC motors through the bevel gear. The hip yawing motors are placed in the body, while the other motors are mounted inside of thighs. The initial state of robot is defined that all the legs are placed on the ground symmetrically along the circumference. The range of joint angles q_{i1}, q_{i2}, q_{i3} of leg i is limited in $(-90°, 90°)$, $(-90°, 150°)$, $(-90°, 150°)$, respectively. The body is covered by a hemispheric shell which can help the robot to return to the original position if it turned over. There are three parts inside of the robot body. The bottom part accommodates the battery and motors. The middle part contains the hardware of control system such as CPU board, motion drive, control cards and video capture card, etc. Binocular camera that can be stretched out of the shell for environmental detection is placed at the top.

This robot can walk in various gaits such as 3 + 3 insect gait, mammal gait and mixed gait. In the insect gait and mammal gait, the legs are parallel to each other in the initial configuration. The motion direction is vertical to the legs in the insect gait as Fig. 2(a), while in the mammal gait the motion direction parallel to the legs as in Fig. 2(b). In the mixed gait as in Fig. 2(c), one leg walks as in the mammal gait and two legs walk as in the insect gait in every half period. There are always three supporting legs during a locomotion cycle. If one or two legs are broken or used as manipulators, the robot can walk in 5 + 1 or 4 + 2 gait [15,16]. In this article the mixed gait is selected as a case to analyze the dynamics and performance of the six-legged robot.

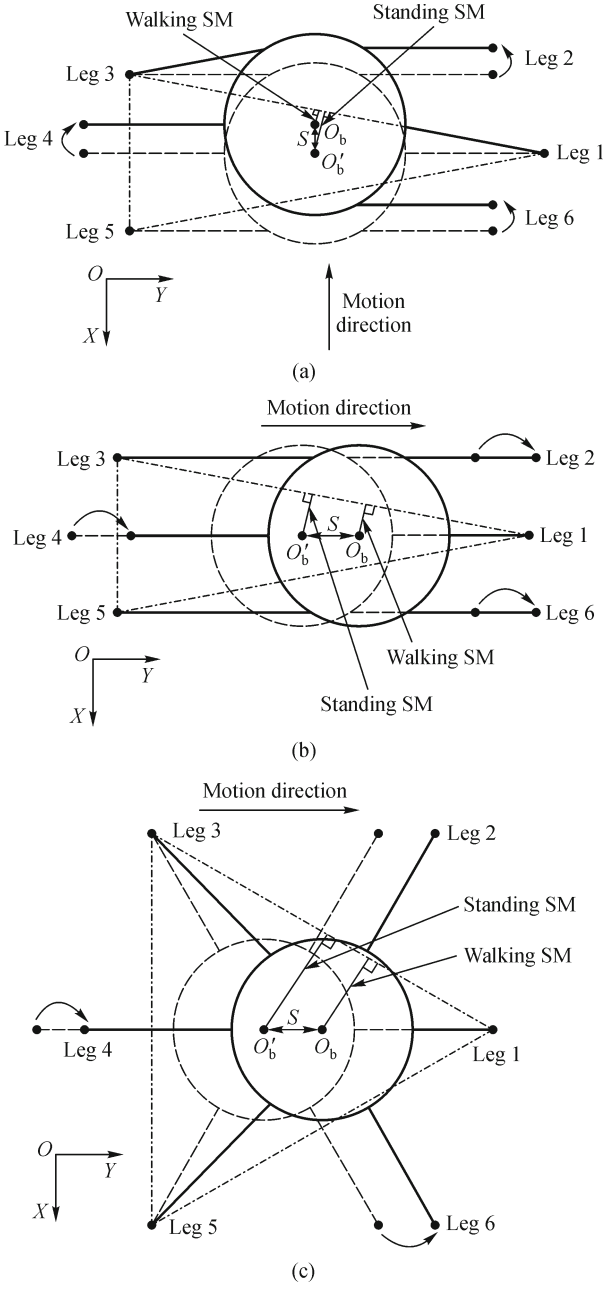

Fig. 2 Different gaits of the radial symmetric six-legged robot (a) Insect gait; (b) mammal gait; (c) mixed gait

As shown in Fig. 2, the dotted line is the initial position

of the robot and the black line is a new position in its motion. In this step the robot is supported by legs 1, 3, 5 and legs 2, 4, 6 are the swinging legs. The supporting area is determined by the position of feet 1, 3, 5. The stability margin (SM) which is the distance between vertical projection of the robot's gravity center and the support polygon changes with the movement of robot. The standing SM of the initial configuration is the largest. Since the supporting area remain unchanged and the body move forward, the walking SM becomes smaller than the standing SM which means that the stability is reduced during walking. If the step length is too large, it may cause the robot turn over especially on the uneven terrain. Therefore the changes of stability should be involved in the analysis of dynamic performance.

2.2 Inverse kinematics of the robot

In order to obtain the joint angles when the robot's feet are constrained to track the predefined paths, the inverse kinematics is necessary.

As shown in Fig. 1, R_b is the radius of body; L_1, L_2 and L_3 are the lengths of hip, thigh and calf; P_{i1c}, P_{i2c}, P_{i3c} are the gravity centers of each link of leg i coinciding with the geometric centers. The robot walks along the axis Y of the inertial coordinate system O-XYZ, the reference coordinate O_b-$X_bY_bZ_b$ is attached to the center of body frame. Vector $\boldsymbol{p}_b = [x_b\ y_b\ z_b]^T$ and three Euler angles (α,β,γ) are selected to represent the global position and posture of the body. The generalized coordinates of body and leg i are $\boldsymbol{q}_b = [p_b\ q_b]^T$ and $\boldsymbol{q}_i = [q_{i1}\ q_{i2}\ q_{i3}]^T$, $i = 1,2,\ldots,6$ respectively, where $\boldsymbol{q}_b = [a\ b\ g]^T$ is the orientation of body in the inertial coordinate system. Thus, the rotation matrix $\boldsymbol{R}$ can be expressed as

$$\boldsymbol{R} = \begin{bmatrix} c\gamma c\alpha - c\beta s\alpha c\gamma & -s\gamma c\alpha - c\beta s\alpha c\gamma & s\beta s\alpha \\ c\gamma s\alpha + c\beta c\alpha s\gamma & -s\gamma s\alpha + c\beta c\alpha c\gamma & -s\beta c\alpha \\ s\beta s\gamma & s\beta c\gamma & c\beta \end{bmatrix}, \quad (1)$$

where c and s refer to cosine and sinus functions, respectively.

Because the trajectories of robot's body and foot are predefined, the position vector of foot tip in O_b-$X_bY_bZ_b$ can be expressed as ${}^b\boldsymbol{p}_{if} = ({}^bx_{if}\ {}^by_{if}\ {}^bz_{if})^T$ given by

$$\boldsymbol{p}_{if} = \boldsymbol{R}^b\boldsymbol{p}_{if} + \boldsymbol{p}_b. \quad (2)$$

Since the plane of leg is perpendicular to X_bY_b plane of the reference coordinate, the mapping of leg i in X_bY_b plane can be described as

$$\begin{aligned} &L_2cq_{i2} + L_3c(q_{i2}+q_{i3}) = \sqrt{{}^bx_{if}^2 + {}^by_{if}^2} - L_1, \\ &L_2sq_{i2} + L_3s(q_{i2}+q_{i3}) = -\,{}^bz_{if}, \\ &\tan(q_{i1}+p/2) = {}^by_{if}/\,{}^bx_{if}. \end{aligned} \quad (3)$$

The joint angles (q_{i1}, q_{i2}, q_{i3}) of leg i can be obtained by solving Eq. (3) [17]. There are two groups of possible solutions for the joints of each leg, but only one of them is chosen as based on the desired configuration of leg i. For example, when the position of foot 1 is given, both q_{i2}, q_{i3} and q'_{i2}, q'_{i3} are the possible solutions as shown in Fig. 3. However, q'_{i2}, q'_{i3} should be abandoned because the knee joints suffer from heavy loads in this case.

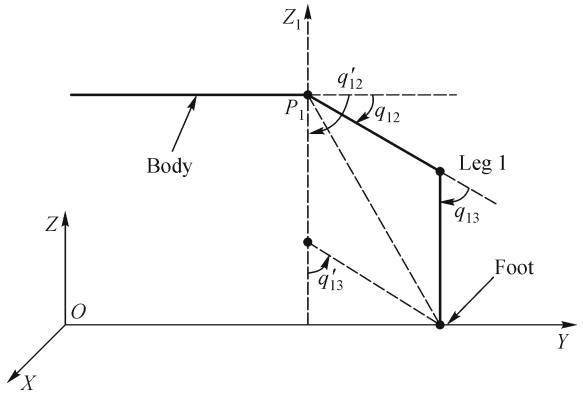

Fig. 3 Two groups of possible solutions for a leg

3 Dynamic modeling of the robot

The six-legged robot can be treated as a floating body with six legs if the constraints between foot and ground are substituted by constraint force vectors. The dynamic equations of the robot system can be developed by Lagrange equations combining the constraint relation between $\boldsymbol{q}_b$ and $\boldsymbol{q}_i$.

The total kinetic energy of the robot system is the sum of the kinetic energy of body and six legs. Based on the generalized coordinate $\boldsymbol{q}_b$, the kinetic energy of body can be expressed as

$$E_{kb} = \frac{1}{2}\dot{\boldsymbol{q}}_b^T\boldsymbol{M}_b\dot{\boldsymbol{q}}_b, \quad (4)$$

where

$$\boldsymbol{M}_b = \begin{bmatrix} m_b & & & & & \\ & m_b & & & & \\ & & m_b & & & \\ & & & I_{bx} & & \\ & & & & I_{by} & \\ & & & & & I_{bz} \end{bmatrix},$$

is the inertia matrix of body. m_b, I_{bx}, I_{by}, I_{bz} are the mass and rotational inertia of the body.

The kinetic energy of one leg is the sum of translational kinetic energy of three links' gravity center and their rotational kinetic energy around each gravity center. Once

the gait is selected the position of each link in the inertial coordinate can be determined as

$$\boldsymbol{p}_{ijc} = \boldsymbol{p}_{b} + \boldsymbol{R}^{b}\boldsymbol{p}_{ijc},\ i = 1,2,...,6,\ j = 1,2,3, \tag{5}$$

where

$$\begin{aligned}
{}^{b}\boldsymbol{p}_{i1c} &= \frac{{}^{b}\boldsymbol{p}_{i2} - {}^{b}\boldsymbol{p}_{i1}}{2} + {}^{b}\boldsymbol{p}_{i1},\\
{}^{b}\boldsymbol{p}_{i2c} &= \frac{{}^{b}\boldsymbol{p}_{i3} - {}^{b}\boldsymbol{p}_{i2}}{2} + {}^{b}\boldsymbol{p}_{i2},\\
{}^{b}\boldsymbol{p}_{i3c} &= \frac{{}^{b}\boldsymbol{p}_{if} - {}^{b}\boldsymbol{p}_{i3}}{2} + {}^{b}\boldsymbol{p}_{i3},
\end{aligned} \tag{6}$$

are the vectors of gravity center of each link of leg i. Leg i can be determined by the position vectors ${}^{b}\boldsymbol{p}_{ij}$ of its joints and foot in the form

$$\begin{aligned}
{}^{b}\boldsymbol{p}_{i1} &= [-R_{b}s\varphi\ \ R_{b}c\varphi\ \ 0]^{T},\\
{}^{b}\boldsymbol{p}_{i2} &= {}^{b}\boldsymbol{p}_{i1} + [-L_{1}sq'_{i1}\ \ L_{1}cq'_{i1}\ \ 0]^{T},\\
{}^{b}\boldsymbol{p}_{i3} &= {}^{b}\boldsymbol{p}_{i2} + [-L_{2}cq_{i2}sq'_{i1}\ \ L_{2}cq_{2}cq'_{i1}\ \ -L_{2}sq_{i2}]^{T},\\
{}^{b}\boldsymbol{p}_{if} &= {}^{b}\boldsymbol{p}_{i3} + [-L_{3}cq_{i3}sq'_{i1}\ \ L_{3}cq_{i3}cq'_{i1} - L_{2}sq_{i2} - L_{3}sq_{i23}]^{T},
\end{aligned} \tag{7}$$

where $q'_{i1} = q_{i1} + \varphi$, $\varphi = (i-1)\dfrac{\pi}{3}$, $q_{i23} = q_{i2} + q_{i3}$.

Velocity of the gravity center of link j of leg i can be obtained by differentiating Eq. (5) with respect to time to get

$$\boldsymbol{v}_{ijc} = \dot{\boldsymbol{p}}_{ijc} = \dot{\boldsymbol{p}}_{b} - \boldsymbol{R}^{b}\hat{\boldsymbol{p}}_{ijc}\boldsymbol{G}\dot{\boldsymbol{q}} + \boldsymbol{R}\boldsymbol{J}_{ij}\dot{q}_{i}, \tag{8}$$

where ${}^{b}\hat{\boldsymbol{p}}_{ijc}$, $\boldsymbol{J}_{ij}$ is the skew symmetric matrix and Jacobian matrix of ${}^{b}\boldsymbol{p}_{ijc}$ respectively. The rotational influence matrix $\boldsymbol{G}$ [18] is

$$\boldsymbol{G} = \begin{bmatrix} s\beta s\gamma & c\gamma & 0\\ s\beta c\gamma & -s\gamma & 0\\ c\beta & 0 & 1 \end{bmatrix}.$$

Rearranging Eq. (8) yields

$$\boldsymbol{v}_{ijc} = \left[\boldsymbol{I}_{3\times 3}\ -\boldsymbol{R}^{b}\hat{\boldsymbol{p}}_{ijc}\boldsymbol{G}\ \boldsymbol{R}\boldsymbol{J}_{ij}\right][\dot{q}_{b}\ \dot{q}_{i}]^{T}. \tag{9}$$

Thus, the kinetic energy of link j of leg i is given by

$$E_{kij} = \frac{1}{2}m_{ij}\boldsymbol{v}_{ijc}^{T}\boldsymbol{v}_{ijc} + \frac{1}{2}j_{ij}\dot{q}_{ij}\dot{q}_{ij}. \tag{10}$$

Substituting Eq. (9) into Eq. (10) yields

$$E_{kij} = \frac{1}{2}\left([\dot{q}_{b}\ \dot{q}_{i}]\boldsymbol{M}_{ij}\begin{bmatrix}\dot{q}_{b}\\ \dot{q}_{i}\end{bmatrix} + j_{ij}\dot{q}_{ij}^{2}\right),$$

where

$$\boldsymbol{M}_{ij} = \begin{bmatrix} m_{ij}\boldsymbol{I} & -\boldsymbol{R}m_{ij}\boldsymbol{G}' & \boldsymbol{R}m_{ij}\boldsymbol{J}_{ij}\\ -\boldsymbol{R}m_{ij}\boldsymbol{G}' & \boldsymbol{G}'^{T}m_{ij}\boldsymbol{G}' & \boldsymbol{G}^{T}m_{ij}\,{}^{b}\hat{\boldsymbol{p}}_{ijc}\boldsymbol{J}_{ij}\\ \boldsymbol{R}m_{ij}J_{ij} & \boldsymbol{G}^{T}m_{ij}\,{}^{b}\hat{\boldsymbol{p}}_{ijc}\boldsymbol{J}_{ij} & m_{ij}\boldsymbol{J}_{ij}^{T}\boldsymbol{J}_{ij} \end{bmatrix},$$

$\boldsymbol{G}' = {}^{b}\hat{\boldsymbol{p}}_{ijc}\boldsymbol{G}$, $\boldsymbol{M}_{ij}$ is the inertia matrix of link j of leg i, and m_{ij}, $\boldsymbol{J}_{ij}$ are the mass and rotational inertia of link j of leg i.

Thus, the kinetic energy of leg i is computed as

$$E_{ki} = \sum_{j=1}^{3} E_{kij}. \tag{11}$$

Therefore, the total kinetic energy of robot system can be expressed as

$$E_{k} = E_{kb} + \sum_{i=1}^{6} E_{ki}. \tag{12}$$

When adopting the mixed gait, the supporting legs and swinging legs alternate between the odd number legs and even number legs. When legs 1, 3, 5 support the body, the Lagrange equations of robot system are

$$\begin{aligned}
&\frac{d}{dt}\left(\frac{\partial E_{k}}{\partial \dot{q}_{0}}\right)^{T} - \left(\frac{\partial E_{k}}{\partial q_{0}}\right)^{T}\\
&= \sum_{i=1}^{3} Q_{q_{b}}^{2i-1} + Q_{b} + \sum_{i=1}^{3}(C_{q_{0}}^{i})^{T}F_{c}^{2i-1},
\end{aligned} \tag{13}$$

$$\begin{aligned}
&\frac{d}{dt}\left(\frac{\partial E_{k}}{\partial \dot{q}_{i}}\right)^{T} - \left(\frac{\partial E_{k}}{\partial q_{i}}\right)^{T}\\
&= \tau_{i} + Q_{q_{i}}^{i} + (C_{q_{i}}^{i})^{T}F_{c}^{i}, i = 1,3,5,
\end{aligned} \tag{14}$$

$$\frac{d}{dt}\left(\frac{\partial E_{k}}{\partial \dot{q}_{i}}\right)^{T} - \left(\frac{\partial E_{k}}{\partial q_{i}}\right)^{T} = Q_{q_{i}}^{i} + \tau_{i}, i = 2,4,6, \tag{15}$$

where $C_{qo}^{i} = \left[\boldsymbol{I} - A^{b}\hat{p}_{if}\boldsymbol{G}\right]$, $C_{q_{i}}^{i} = A\boldsymbol{J}_{if}$.

Eqs. (13)–(15) are the dynamic equations as referring to robot body, legs in contact with ground, and legs in swinging phase, respectively. $Q_{q_{b}}^{i}$, $Q_{q_{i}}^{i}$ are the generalized forces for the generalized coordinates of body and leg i due to the mass of leg i respectively, Q_{b} is the generalized force due to the gravity of body [1]. F_{c}^{i} is the constraint force on the foot of supporting leg i which can be determined by force distribution optimizing methods [19–21]. In this paper, the constraint force is calculated based on the simplified model by regarding the foot tips as the spherical hinges.

When the supporting legs change to legs 2, 4, 6, the generalized force and constraint force $\sum_{i=1}^{3} Q_{q_{b}}^{2i-1}$, $\sum_{i=1}^{3} F_{c}^{2i\text{-}1}$

in Eq. (13) change to $\sum_{i=1}^{3} Q_{q_b}^{2i}$, $\sum_{i=1}^{3} F_c^{2i}$ and the number i in Eqs. (14) and (15) is switched.

Moreover, q_b and q_i are dependent due to the contact constraints between the foot and ground. When the trajectory of foot p_{if} (t) is given, the constraint equation can be expressed as

$$^{b}\boldsymbol{p}_{if} = \boldsymbol{R}^{T}(\boldsymbol{p}_{if} - \boldsymbol{p}_{b}),\ i = 1,2,...,6,\ j = 1,2,3. \tag{16}$$

Rearranging and differentiating Eq. (16) with respect to time can give expressions for $\dot{q}_i$, $\ddot{q}_i$. The complete dynamic equations can be obtained when $\dot{q}_i$ and $\ddot{q}_i$ are expressed by q_b through the constraint equations together with the dynamic Eqs. (13)–(15).

The proposed dynamic modeling is formulated to characterize the operation of the robot but also to evaluate its dynamic performance through numerical simulation results.

4 An index for total torque

In order to analyze the dynamic performance of the six-legged robot, indices just considering the energy consumed are not comprehensive. Robot stability should also be considered, because the parameters of robot which minimize the power consumption may reduce the stability excessively.

The stability of the radial symmetric six-legged robot is measured by SM as described in Sect. 2. To increase the stability, the supporting feet should be located far away from the body. However, the position of a supporting foot on the *O-XY* plane may occur inside the area of body's projection during a step due to the unpredicted situations such as excessive step length, length distribution of thigh and calf etc. An example is shown in Fig. 4 where the initial position and posture of body and leg 1 are depicted in bold dotted lines, while their final position and posture are represented in bold solid lines. P_{1XY} and P'_{1XY} are the projection of P_1 and P'_1 on the ground. As can be seen in Fig. 4(a), the foot is outside of the projection area of body during the step, while in Fig. 4(b) the foot appears between P_{1XY} and P'_{1XY} inside of the area of body's projection and the stability of the robot is poor. Therefore Fig. 4(a) is a desired posture but Fig. 4(b) is unexpected in a locomotion cycle. It is fairly easy to find that once the supporting leg 1 reaches on undesired posture, the direction of τ_{12} will change, i.e., the sign of its value will change.

Thus, in order to prevent a reduction of robot's stability, a novel index of total torque is proposed by considering the posture of supporting legs as

$$T_{tot} = \sum_{i=1}^{6}\sum_{j=1}^{3}\sum_{k=1}^{n}\frac{T}{n}\left|\tau_{ij}(t_k)\right|, \tag{17}$$

with

$$\tau_{i2}(t_{k+1}) = \begin{cases} \tau_{i2}(t_{k+1}), & \tau_{i2}(t_k)\tau_{i2}(t_{k+1}) \geqslant 0, \\ M_f\tau_{i2}(t_{k+1}), & \tau_{i2}(t_k)\tau_{i2}(t_{k+1}) < 0, \end{cases},$$

where T_{tot} is the sum of all $i \times j$ joint torques in a periodic time T, i is the number of leg and j is the number of joints of a leg. Torques τ_{ij} of the hip yawing joints and knee joints are measured every T/n seconds. If the robot walks in a stable posture as in Fig. 4(a), the measured torques τ_{ij} of

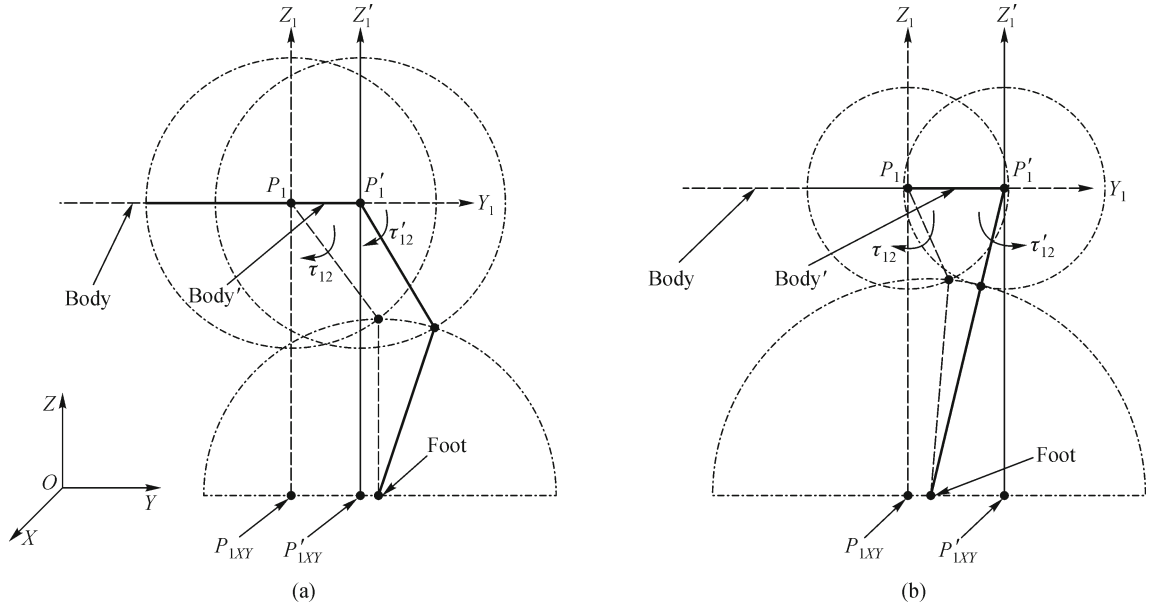

Fig. 4 The posture of supporting leg 1
(a) Stable posture; (b) unstable posture

hip pitching joints can be applied directly. In an undesired posture, however, the torque of hip pitching joint $\tau_{i2}(t_{k+1})$ will be amplified by magnification factor M_f ($M_f \gg 0$) when its direction become opposite to $\tau_{i2}(t_k)$. The optimal values of torques can be based on this index and the minimum T_{tot} can be properly used.

A comparative simulation experiment is reported to show its validity. Based on the inverse dynamics, the index of density of power lost (T_L) in Ref. [5] and torque considering the posture of supporting legs (T_{tot}) for six examples of leg design (LD1–LD6) as in Table 1 are evaluated, where L_2, L_3 are the length of thigh and calf, respectively.

Table 1 Six examples of leg design

	LD1	LD2	LD3	LD4	LD5	LD6
L_2/mm	300	270	100	200	150	230
L_3/mm	300	330	500	400	450	370

Let the general coordinates $q_{i1} = 0°$, $q_{i2} = 30°$, $q_{i3} = 60°$ at the standing state, the robot walks along the direction of leg 1 (parallel to Y-axis) in the mixed gait, legs 1, 3, 5 are the supporting legs at the beginning. The step length is S = 100 mm, and cycle time is T = 2 s. The height of body is unchanged during the motion.

Let's consider the above notation with:
m_b = 30 kg, m_1 = 0.5 kg, m_2 = 2 kg, m_3 = 2.5 kg, R_b = 300 mm, L_1 = 150 mm, L_2 = 300 mm, L_3 = 300 mm, I_{bx} = 0.7 kg·m^2, I_{by} = 0.7 kg·m^2, I_{bz} = 1.35 kg·m^2, $j_{12} = j_{13}$ = 0.015 kg·m^2, M_f = 200, n = 10.

Taking leg 1 as an example, the torque value of τ_{12}, τ_{13} for all examples of leg design in a periodic locomotion are shown in Fig. 5. As can be seen in Fig. 5(a), all the lines of torque of hip pitching joint change smoothly except line 3. There is a numerical mutation of τ_{12} for LD3, because the thigh is too much short in this case, and the supporting leg 1 cannot be allocated a series of continuous rotation angles to follow foot's path. The sudden variation of torque from about 10 N·m to −90 N·m suddenly may cause serious damage to the motor. Torque of hip pitching joint for LD1 is the maximum during a step, while torque for LD5 is the minimum. However, in LD5 τ_{12} change into negative value at the end of the step which indicates that the supporting leg is located in the unstable posture as in Fig. 4(b). Therefore, both of LD3 and LD5 are not the feasible choices. Torque of knee joint for LD3 is the maximum, while torque for LD1 is the minimum as shown in Fig. 5(b). The variation trend of all lines maintain uniform,

To obtain the optimal design among LD1–LD6, performance index T_L and T_{tot} are employed here. The results of T_L and T_{tot} are calculated as based on τ_{12}, τ_{13} and illustrated in Fig. 6. According to the result of index T_L, Example 5 is the optimal design since its value is the minimum as in Fig. 6(a). From Fig. 6(b), however, the minimum T_{tot} is related to Example 4 as based on the

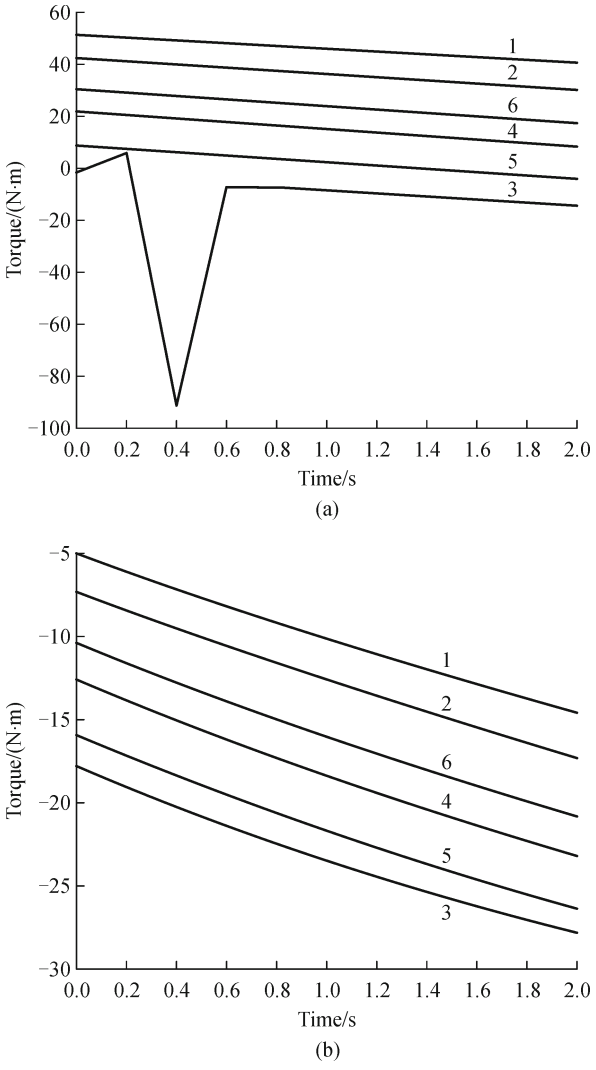

Fig. 5 The joint torques during motion of leg 1
(a) The torque of hip pitching joint; (b) the torque of knee joint

Eq. (17). The optimal solutions according to these two indices are different. Because the length distribution of thigh and calf in LD3 and LD5 cause the unstable posture during one step, the τ_{12} for these two cases had been amplified by the magnification factor M_f in index T_{tot}.

Simulation results show that the index T_L can be used for optimizing the design parameters of leg to fullfile the goal of consuming minimum energy, but it can't avoid the unexpected posture of supporting legs. While the index T_{tot} not only can reject the design parameters causing the unstable posture, but also find the optimal design of leg with minimum energy consumption.

5 Analysis of the robot's dynamic performance

In order to characterize robot dynamic performance a parametric study has been carried out by simulating its

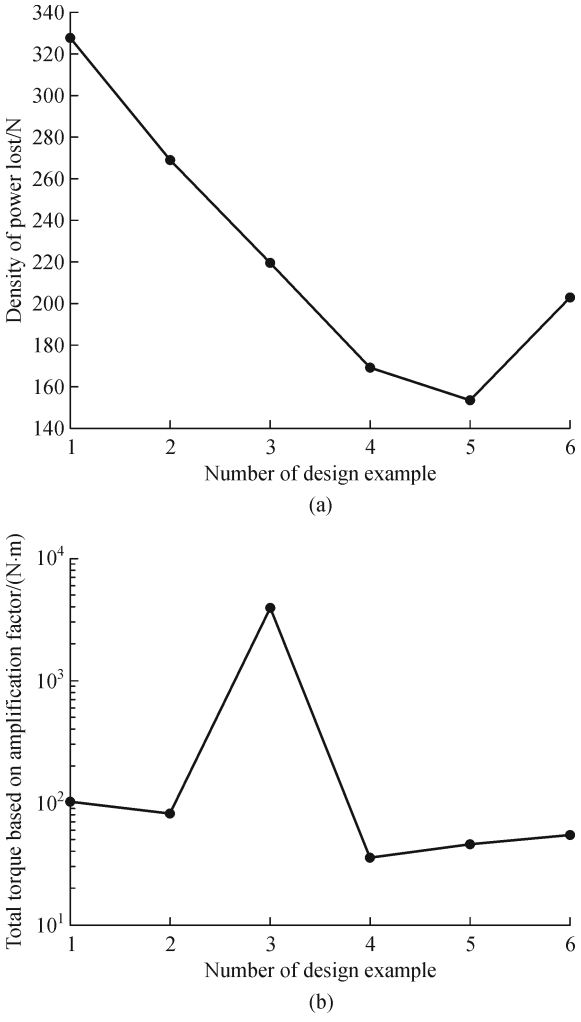

Fig. 6 Value of index T_L and T_{tot} for six design examples (a) Index T_L; (b) index T_{tot}

operation for different design conditions. Results are summarized in the following.

5.1 The effect of design parameters

Four important parameters are selected to analyze their influence on joint torques, namely the length of leg (L_2, L_3), the mass distribution of leg (m_2, m_3), the step length (S), and the joint angles of supporting legs in standing state (q_{ij}). Since the dynamics of swinging legs has been well studied when it is treated as mobile manipulators [22–24], we have just analyzed the dynamics of supporting legs.

The motion and notations of the robot are same with those in Sect. 4. The normal values of these four parameters are L_2 = 300 mm, L_3 = 300 mm; m_2 = 2 kg, m_3 = 2.5 kg; S = 100 mm; q_{i1} = 0, q_{i2} = 30°, q_{i3} = 60° at the standing state.

Taking leg 1 as an example, the torques of hip pitching joint (τ_{12}) and knee joint (τ_{13}) for normal values of the parameters are displayed by the line 1 in Figs. 7–10 as results of numerical simulations. The average value of τ_{12} and τ_{13} are 46 N·m and −10 N·m respectively. To illustrate the effect of these four parameters, joint torques are also calculated in the condition that one parameter changes at a rate of 10% and 20%, meanwhile, the other two parameters remain unchanged.

Figure 7 shows the variation of τ_{12} and τ_{13} for five different lengths of L_2 and L_3 as in Table 2. From the simulation results, in one step, the variation trend of τ_{12} or τ_{13} for five cases in one step keep almost uniform. The τ_{12} for case 5 is the maximum during a step, while it is the minimum for case 3. On the contrary, the τ_{13} for case 5 is the minimum but the maximum for case 3. Difference between the adjacent lines in Fig. 7(a) is about 9 N·m, and that is 2.5 N·m in Fig. 7(b), which means that 10% variation of L_2 and L_3 cause τ_{12} and τ_{13} to change 20% and 40% respectively.

Table 2 Different lengths of L_2 and L_3

	Case 1	Case 2	Case 3	Case 4	Case 5
L_2/mm	300	270	240	330	360
L_3/mm	300	330	360	270	240

Figure 8 shows the result of τ_{12} and τ_{13} for different groups of m_2 and m_3 in Table 3. The variation trend of the five lines which are the torques of hip pitching joint (τ_{12}) for five different distributions of leg's mass keep uniform in Fig. 8(a). Torque τ_{12} for case 3 is the maximum, while its minimum value is for case 5. The result of Fig. 8(a) is just opposite to Fig. 7(a). Difference between the adjacent lines in Fig. 8(a) is about 0.2 N·m, which means 10% variation of m_2 cause τ_{12} just to change 0.43%. Furthermore, the torque of knee joints τ_{13} almost keep unchanged for the five cases of legs' mass distribution. The effect of mass distribution of leg on the joint torques is little because the body of robot (30 kg) is much heavier than one leg.

The effect of different step length is shown in Fig. 9. Line 2 and line 3 describe the torque in the situation of S = 90 mm, S = 80 mm, while line 4 and line 5 represent the torque for S = 110 mm, S = 120 mm. The five cases have the same initial value of both τ_{12} and τ_{13}, but their values change over time. The τ_{12} decreases gradually, while the τ_{13} increases in the opposite direction. The maximum variation of both joint torques are about 1Nm at the end of lines, which suggest the changes of τ_{12}, τ_{13} are 2.2% and 10% caused by 10% variation of step length.

The effect of the joint angles in standing state to τ_{12} and τ_{13} is illustrated in Fig. 10. The line 2 and line 3 represent the torque in the situation of q_{i2} = 33°, q_{i2} = 36°, while line 4 and line 5 describe the torque for q_{i2} = 27°, q_{i2} = 24°. To maintain the calf being perpendicular to the ground in standing state, $q_{i3} = 90° - q_{i2}$. The variation trends of five lines are also uniform. The difference of τ_{12} is about

Table 3 Different groups of m_2 and m_3 /kg

	Case 1	Case 2	Case 3	Case 4	Case 5
m_2/kg	2	1.8	1.6	2.2	2.4
m_3/kg	2.5	2.7	2.9	2.3	2.1

Table 4 The effect of different parameters to the joint torques of supporting legs

	10% change of L_2 and L_3	10% change of m_2 and m_3	10% change of step length	10% change of joint angles
τ_{12} change	20%	0.43%	2.2%	4.3%
τ_{13} change	40%	Neglect	10%	Neglect

2 N·m, which means that 10% variation of q_{i2} lead a change of 4.3% of τ_{12}. The difference of τ_{13} is small enough to be neglected.

Based on the simulation results, the effect of different parameters on the joint torques of supporting legs is listed in Table 4. The results show that the change of leg length has great influence, especially on τ_{13}. On the contrary, the effects of mass distribution of a leg and joint angles are relatively less. The influence of step length on the knee joint is significantly greater than hip pitching joins. The results provide a basis for optimizing the leg's structure and operation.

5.2 Analysis of leg operation

In this subsection the leg operations are analyzed in two cases, namely the robot walks with maximum step length

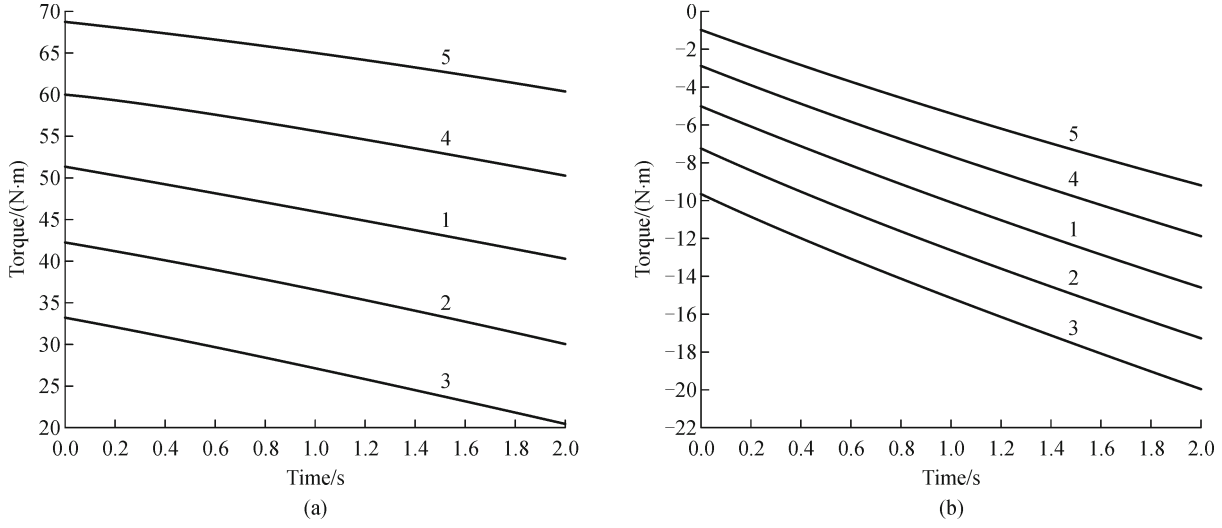

Fig. 7 Results of simulation for different length of leg
(a) Torque of hip pitching joint; (b) torque of knee joint

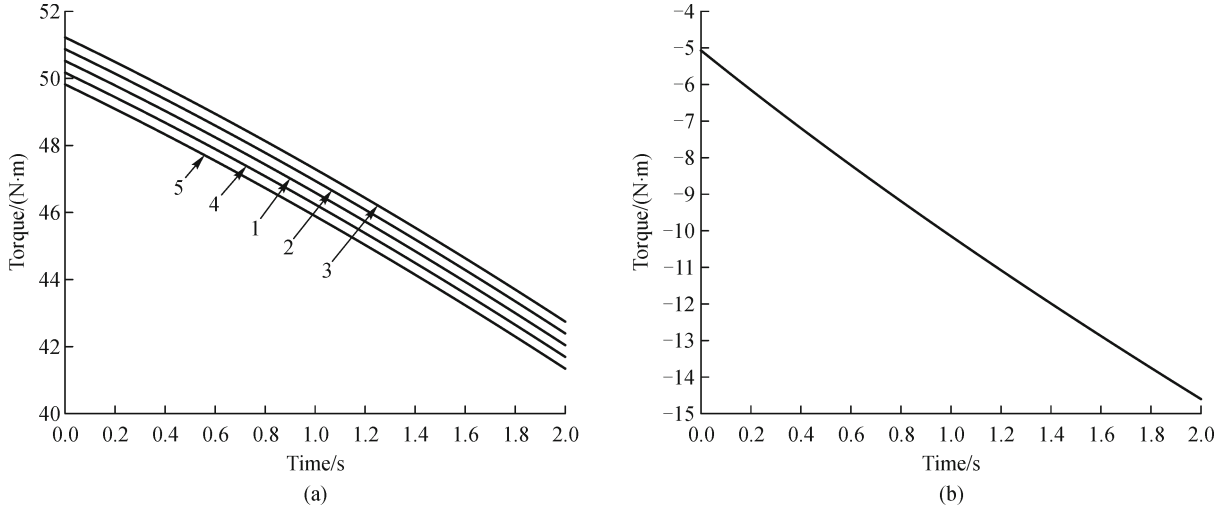

Fig. 8 Results of simulation for different mass distribution of leg
(a) Torque of hip pitching joint; (b) torque of knee joint

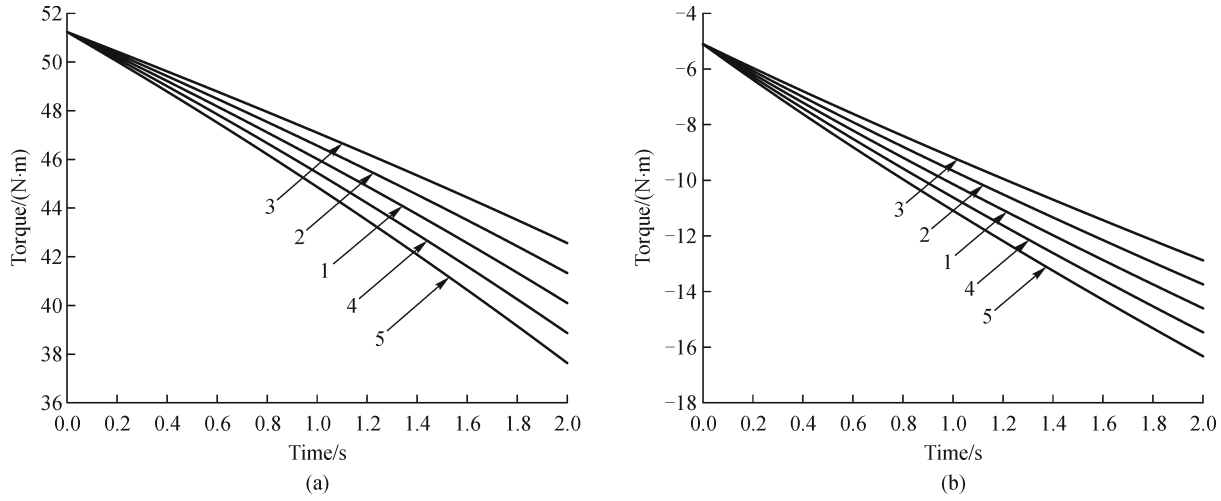

Fig. 9 Results of simulation for different step length
(a) Torque of hip pitching joint; (b) torque of knee joint

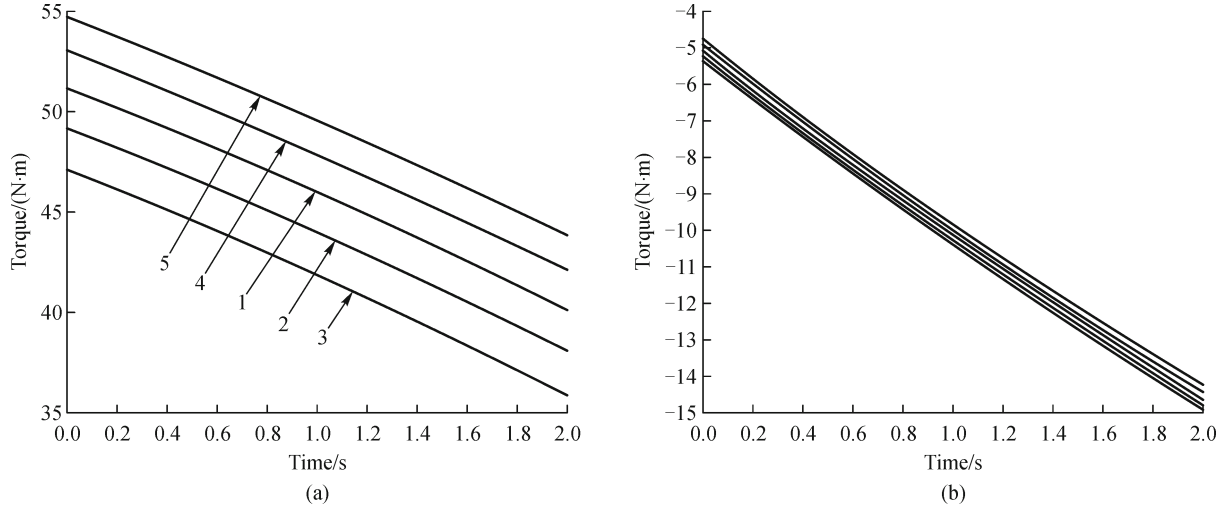

Fig. 10 Results of simulation for different posture of supporting legs
(a) Torque of hip pitching joint; (b) torque of knee joint

with different poses, and it walks with different step length with the same pose.

5.2.1 Maximum step length with different poses

Let's consider the robot walking under the following conditions. In the original standing state, the calves are perpendicular with the ground. The robot walks along the direction of leg 1 in the mixed gait, legs 1, 3, 5 support the robot in the first step. Four different poses of the robot are selected as shown in Fig. 11. The angles between the body and thigh are different in these poses. The robot walks with maximum step length (S_{max}) which is the distance between the foot in state of stand and the projection of P_1 on the ground. The time spent in one step is 2 s with a uniform step frequency in the four situations and the height of body is unchanged during the motion.

Using the dynamic Eq. (14), τ_{12} and τ_{13} are calculated in these four situations. The values of T_{tot} in one step and T_{tot} of per meter are listed in Table 5 as obtained from the numerical simulation. Both S_{max} and T_{tot} in pose Fig. 11(a) are the largest in these four sets of results, while the time spent is the shortest. On the contrary, S_{max} and T_{tot} in pose Fig. 11(c) are the smallest but the walk time is the longest. When the robot stands in its highest state like pose Fig. 11(d), it is not suitable to walk because its foot is located inside of the projection of the body on the ground, so that the stability margin is reduced greatly. The results demonstrate that both the total torque and time spent per meter in these four cases are different according to the

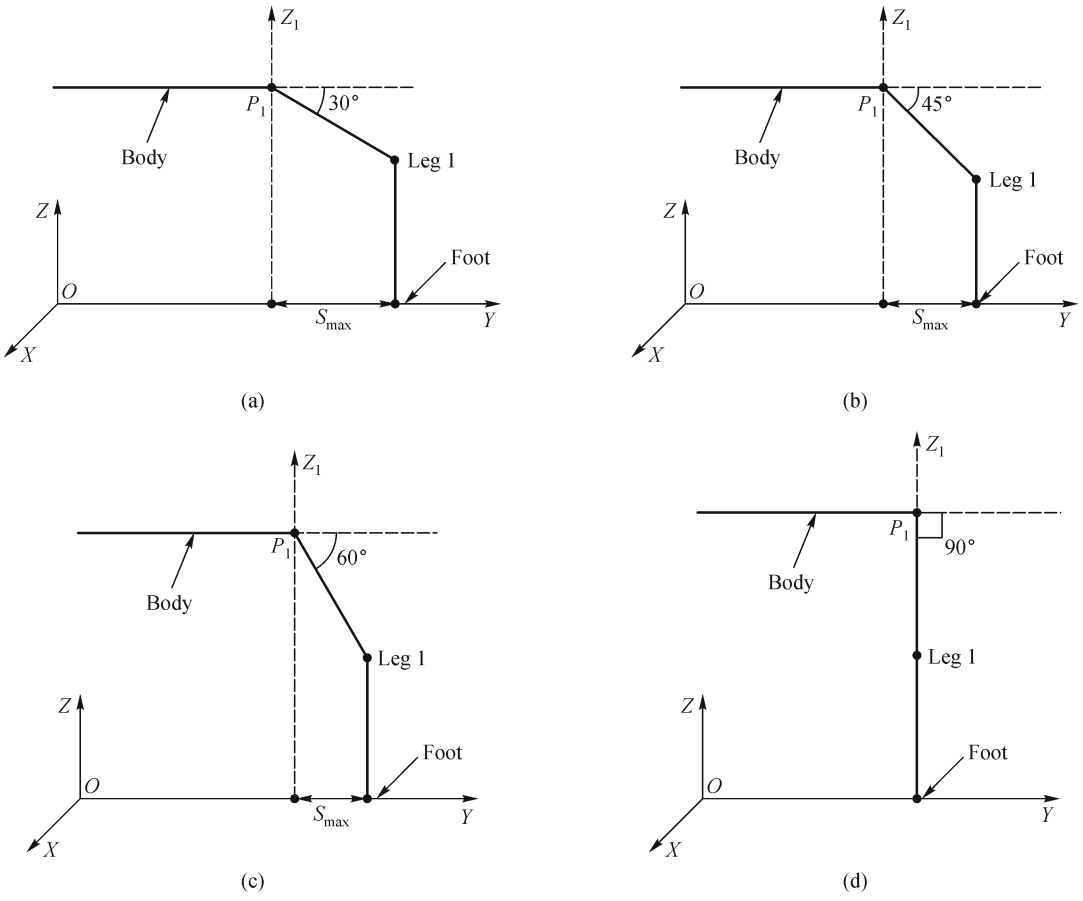

Fig. 11 The robot walks in four different poses
(a) Pose 1; (b) pose 2; (c) pose 3; (d) pose 4

Table 5 Results form numerical simulation for total torque and time spent in four different poses

	S_{max}/m	T_{tot} of one step	T_{tot} of per meter	Time spent per meter/s
Pose 1	0.260	93.4	359.23	7.7
Pose 2	0.212	70.6	333.02	9.4
Pose 3	0.150	41.7	278.00	13.3
Pose 4	0	0	0	∞

above conditions. Therefore, when the robot stand higher, the total torque consumed per meter is lower but the time spent is longer. While the robot's height is lower, the T_{tot} of per meter becomes larger and the time spent is shorter.

5.2.2 Different step length with the same pose

Let's consider the robot also walking along the direction of leg 1 in the mixed gait as shown in Fig. 12. The dotted line is the initial position of leg 1 and the black line is its final position in a step. Four different step lengths S_1–S_4 are selected to analyzed the robot dynamic performance. The step frequency in the situations is uniform, and the height of body also remains unchanged during the motion in each case.

The results of T_{tot} and the time spent per meter are listed in Table 6. The smallest value of T_{tot} and time spent per meter appear in case Fig. 12(a), and the largest T_{tot} and time spent per meter appear in case Fig. 12(d). The results demonstrate that the total torque consumed and the time spent per meter in the same pose of robot are determined by the step length. The value of T_{tot} and the time spent per meter are inversely proportional to the step length. In order to consuming minimum power and spending the shortest time, the robot should walk with the maximum step. Meanwhile, the stability of case Fig. 12(a) is the worst among these four cases.

6 Conclusions

In this paper the dynamic performance of a radial symmetric six-legged robot has been analyzed. The dynamic model of the robot has been formulated according to the Lagrange equations. A new index of total torque has been proposed by considering the posture of supporting legs (T_{tot}), and its validity has been verified by comparing

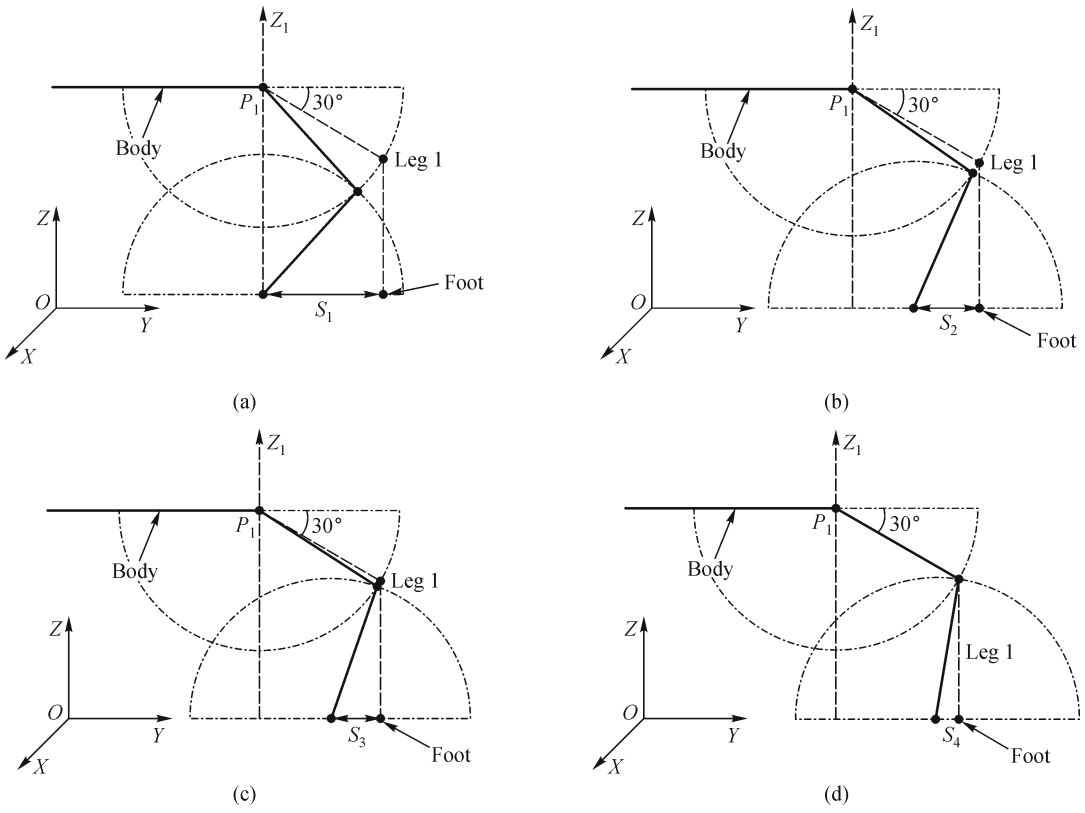

Fig. 12 The robot walks by four different step lengths
(a) S_1; (b) S_2; (c) S_3; (d) S_4

Table 6 Results form numerical simulation for total torque and time spent in the same pose

	Step length/m	T_{tot} of one step	T_{tot} of per meter	Time spent per meter
S_1	0.260	93.4	359.23	7.7
S_2	0.130	107.8	829.23	15.4
S_3	0.087	111.9	1286.20	23.0
S_4	0.043	115.8	2693.00	46.5

the simulation results with the existing index T_L. The index T_{tot} can be used to identify the optimal design of robot for minimizing energy consumption and preventing the unstable posture.

Results of the analysis of dynamic performance show that the change of leg length has great influence on the joint torques of supporting legs, yet the effect of joint angles is relatively less. Moreover, the influence of step length on the knee joint is significantly greater than it on hip pitching joint. When the robot walks in the same step length but different poses, the total torque is determined by S_{max} and T_{tot} of one step. If the robot stands higher, the total torque consumed per meter is lower but the time spent is longer. Else if the robot's height is lower, the T_{tot} of per meter becomes larger and the time spent is shorter. When the robot walks in the same pose but different step lengths, the value of T_{tot} and time spent per meter are inversely proportional to the step length.

Our work in this article is significant to optimize the parameter design of mechanical structure and the leg operation of the radial symmetric six-legged robot.

Acknowledgements This research work was supported by the National Outstanding Youth Science Foundation (No. 51125020).

References

1. Chen W J, Yao S H, Low K H. Modular formulation for dynamics of multi-legged robots. In: Proceedings of the 8th International Conference on Advanced Robotics, 1997, 279–284
2. Barreto J P, Trigo A, Menezes P, Dias J, Almeida A T. FBD—The free bodydiagram method. Kinematic and dynamic modeling of a six leg robot. International Workshop on Advanced Motion Control, 1998, 423–428
3. Yiu Y K, Cheng H, Xiong Z H, Liu G F, Li Z X. On the dynamics of parallel manipulators. In: Proceedings of IEEE International Conference on Robotics and Automation, 2001, 4: 3766–3771
4. Ding X L, Li K J, Xu K. Dynamics analysis of six-legged robot with elastic joints using screw theory. Journal of Central South University (Science and Technology), 2011, 42: 589–595

5. Silva M F, Tenreiro Machado J A. Kinematic and dynamic performance analysis of artificial legged systems. Robotica, 2008, 26(1): 19–39
6. Bowling A. Mobility and dynamic performance of legged robots. In: proceedings of the IEEE International Conference on Robotics and Automation, 2005, 4100–4107
7. Bowling A. Dynamic performance, mobility, and agility of multi-legged robots. Journal of Dynamic Systems, Measurement, and Control, 2006, 128(4): 765–777
8. Erden M S, Leblebicioglu K. Torque distribution in a six-legged robot. IEEE Transactions on Robotics, 2007, 23(1): 179–186
9. Low K H, Bai S P. Terrain-evaluation-based motion planning for legged locomotion on irregular terrain. Advanced Robotics, 2003, 17(8): 761–778
10. Bai S P, Low K H, Zielinska T. Quadruped free gait generation for straight‐line and circular trajectories. Advanced Robotics, 1998, 13(5): 513–538
11. Carbone G, Shrot A, Ceccarelli M. Operation strategy for a low-cost easy-operation Cassino Hexapod. Applied Bionics and Biomechanics, 2008, 4(4): 149–156
12. Carbone G, Suciu M, Ceccarelli M, Pisla D. Design and simulation of cassino hexapode walking machine. International Journal of Mechanics and Control, 2009, 10(2): 27–34
13. Rodriguez N, Eduardo N. A New Design for Cassino hexapod Robot. In: Proceedings of the ASME 10th Biennial Conference on Engineering Systems Design and Analysis (ESDA2010), 2010, 3: 1–6
14. Zielinska T, Heng J. Development of a walking machine: mechanical design and control problems. Mechatronics, 2002, 12 (5): 737–754
15. Wang Z Y, Ding X L, Rovetta A. Analysis of typical locomotion of a symmetric hexapod robot. Robotica, 2010, 28(6): 893–907
16. Wang Z Y, Ding X L, Rovetta A, Giusti A. Mobility analysis of the typical gait of a radial symmetrical six-legged robot. Mechatronics, 2011, 21(7): 1133–1146
17. Chen X D, Sun Y, Jia W C. Motion Planning and Control of Multilegged Walking Robots. Wuhan: Huazhong University of Science and Technology Press, 2006 (in Chinese)
18. Roberson R E. Dynamics of Multibody Systems. New York: Springer-Verlag, 1988, 475
19. Agarwal A, Gautam P, Roy S. Dynamic modeling and optimal foot force distribution of quadruped walking robot. Trends in Intelligent Robotics, Communications in Computer and Information Science, 2010, 103: 146–153
20. Gardner J F. Efficient computation of force distributions for walking machines on rough terrain. Robotica, 1992, 10(5): 427–433
21. Zhou D B, Low K H, Zielinska T. An efficient foot‐force distribution algorithm for quadruped walking robots. Robotica, 2000, 18(4): 403–413
22. Yamamoto Y, Yun X P. Effect of the dynamic interaction on coordinated control of mobile manipulators. International Conference on Robotics and Automation, 1996, 12: 816–824
23. White G, Bhatt R, Tang C, Krovi V. Experimental evaluation of dynamic redundancy resolution in a nonholonomic wheeled mobile manipulator. IEEE/ASME Transactions on Mechatronics, 2009, 14 (3): 349–357
24. Eslamy M, Moosavian S. Dynamics and cooperative object manipulation control of suspended mobile manipulators. Journal of Intelligent and Robotic Systems: Theory and Applications, 2010, 60(2): 181–199